Optimal IIR Filter Design using Novel Particle Swarm Optimization Technique

Suman Kumar Saha, Rajib Kar, Durbadal Mandal, Sakti Prasad Ghoshal

Abstract—This paper demonstrates the application of an evolutionary heuristic search technique called Novel Particle Swarm Optimization (NPSO) for the optimal design of 6th and 8th order low pass and band pass Infinite Impulse Response (IIR) filters. Conventional particle swarm optimization (PSO) has been modified with the attractive features of cognitive information, (*pbest* and *pworst*) and named as NPSO. NPSO helps to speed up the convergence by means of non-advancement of particle to *pworst* position. It finds near optimal solution in terms of a set of filter coefficients. The effectiveness of this algorithm is justified with a comparative study of some well established algorithms, namely, Real coded Genetic Algorithm (RGA) and conventional Particle Swarm Optimization (PSO) with a superior outcome for the designed 6th and 8th order IIR low pass and band pass filters. Simulation results affirm that the proposed NPSO algorithm outperforms its counterparts not only in terms of quality output i.e. sharpness at cut-off, pass band ripple and stop band attenuation but also in convergence speed with assured stability.

Keywords— IIR Filter; RGA; PSO; NPSO; Evolutionary Optimization Techniques; Magnitude Response; Pole-Zero Plot; Stability, Low Pass Filter, Band Pass Filter.

I. Introduction

THE The scientific and technological blossoming of signal processing explores the plethoric requirement of filters as an integral part of all signal processing systems. Application of the filter is not only widely covered but also deeply rooted in its domain of utilization. Application is ranging from ripple reduction of a very simple rectifier circuit to highly sophisticated application zones of biological and astrological signal analysis along with noise reduction of raw signal, video signal enhancement and graphic equalization in hi-fi systems. Basically, a filter is a frequency selective device which extracts the useful portion of input signal lying within its operating frequency range that could be contaminated with random noise due to unavoidable circumstances. On the basis of physical makeup and the way filtration is done, filters can be broadly classified as analog and digital ones. Analog filters are made up with discrete components like resistor, capacitor, inductor and op-amp. Discrete component dependent design, prone to high component tolerance sensitivity, poor accuracy, highly susceptible to thermal drift and large physical size are the major retractions of analog filter implementation. On the contrary, digital filter performs mathematical operation on a sampled, discrete timed signal to achieve the desired features with the help of a specially designed digital signal processor (DSP) chip or a processor used in a general purpose computer.

Digital filters are broadly classified into two main categories namely; finite impulse response (FIR) filter and infinite impulse response (IIR) filter [1-2]. The output of FIR filter depends on present and past values of input, so the name non-recursive is aptly suited to this filter. On the other hand, the output of IIR filter depends not only on previous inputs, but also on previous outputs with impulse responses continuing forever in time at least theoretically, so the name recursive is aptly suited to this filter; anyway, a large memory is required to store the previous outputs for the recursive IIR filter.

Hence, due to these aspects FIR filter realization is easier with the requirement of less memory space and design complexity. Ensured stability and linear phase response over a wide frequency range are the additional advantages. On the other hand, IIR filter distinctly meets the supplied specifications of sharp transition width, less pass band ripple and more stop band attenuation with ensured lower order compared to FIR filter. As a consequence, properly designed IIR filter can meet the magnitude response close to ideal and more finely as compared to FIR filter. Due to these challenging features with wide field of applications, performances of IIR filters designed with various evolutionary optimization algorithms are compared to find out the optimization effectiveness of the algorithms and the best optimal IIR filters.

In the conventional approach, IIR filters of various types (Butterworth, Chebyshev and Elliptic etc.) can be implemented with two methods. In the first case frequency sampling technique is adopted for Least Square Error [3] and Remez Exchange [4] process. In the second method, filter coefficients and minimum order are calculated for a prototype low pass filter in analog domain which is then transformed to digital domain with bilinear transformation. This frequency mapping works well at low frequency, but in high frequency domain this method is liable to frequency warping [5].

IIR filter design is a highly challenging optimization problem. Gradient based classical algorithms such as steepest descent

Manuscript received May 08, 2012.

Suman K Saha, *Rajib Kar, Durbadal Mandal are with Department of Electronics and Communication Engg., National Institute of Technolgy, Durgapur, India (* Corresponding author: Phone: +91-9434788056; fax: +91-343-2547375; e-mail: rajibkarece@gmail.com).

Sakti Prasad Ghosal is with Department of Electrical Engg., National Institute of Technolgy, Durgapur, India. (e-mail: spghoshalnitdgp@gmail.com).

and quasi Newton algorithms had been used for the design of IIR filters [6-7]. In general, these algorithms are very fast and efficient to obtain the optimum solution of the objective function for a unimodal problem. But the error surface (typically the mean square error between the desired response and estimated filter output) of IIR filter is multimodal and hence superior optimization techniques are required to find out better near-global optimal filter designs.

The shortfalls of classical optimization techniques for handling the multimodal optimization problem are as follows: i) Requirement of continuous and differentiable error fitness function (cost or objective function), ii) Usually converges to the local optimum solution or revisits the same sub-optimal solution, iii) Incapable to search the large problem space, iv) Requirement of the piecewise linear cost approximation (linear programming), v) Highly sensitive to starting points when the number of solution variables are increased and as a result the solution space is also increased.

So, owing to the various shortfalls of classical optimization techniques as mentioned above, various evolutionary meta-heuristic algorithms have recently been applied for obtaining better and better optimal filter designs. The algorithms are as follows: Genetic Algorithm (GA) is inspired by the Darwin's "Survival of the Fittest" strategy [8-9]; Simulated Annealing (SA) is designed from the thermodynamic effects [10]; Artificial Immune Systems (AIS) mimics the biological immune systems [11]; Ant Colony Optimization (ACO) simulates the ants' food searching behaviour [12]; Bee Colony Optimization mimics the honey collecting behaviour of the bee swarm [13]; Cat Swarm Optimization(CSO) is based upon the behaviour of cats for tracing and seeking of an object [14]; and Particle Swarm Optimization (PSO) simulates the behaviour of bird flocking or fish schooling [15]-[18].

Naturally, it is a vast area of research continuously being explored for years. In this paper, the capabilities of global searching and near optimum result finding features of GA, PSO and NPSO are investigated thoroughly for solving 6th and 8th order IIR filter design problems. GA is a probabilistic heuristic search optimization technique developed by Holland [19]. The features such as multi-objective, coded variable and natural selection made this technique distinct and suitable for finding the near global solution of filter coefficients.

Particle Swarm Optimization (PSO) is swarm intelligence based algorithm developed by Eberhart *et al.* [20]-[21]. Several attempts have been taken to design digital filter with basic PSO and its modified versions [15], [22-23]. The main attraction of PSO is its simplicity in computation and a few numbers of steps are required in the algorithm.

The limitations of the conventional PSO are premature convergence and stagnation problem [24]-[25]. To overcome these problems an improved version of PSO, called NPSO is suggested by the authors for the design of IIR low pass (LP) and band pass (BP) filters.

The paper is organized as follows: section II describes the IIR filter design problem. Different evolutionary algorithms namely, RGA, PSO and NPSO are discussed in section III. Section IV consists of comprehensive and demonstrative sets of data and illustrations that articulate the usefulness of paper in terms of result and discussion. Finally section V concludes the paper.

II. IIR Filter Design Formulation

This section discusses the design strategy of IIR filter based on NPSO. The input-output relation is governed by the following difference equation [2]:

$$y(p)+\sum_{k=1}^{n}a_k y(p-k)=\sum_{k=0}^{m}b_k x(p-k)$$

where $x(p)$ and $y(p)$ are the filter's input and output, respectively, and $n(\geq m)$ is the filter's order. With the assumption of coefficient $a_0 = 0$, the transfer function of the IIR filter is expressed as:

$$H(z)=\frac{\sum_{k=0}^{m}b_k z^{-k}}{1+\sum_{k=1}^{n}a_k z^{-k}} \quad (1)$$

Let $z=e^{j\Omega}$. Then, the frequency response of the IIR filter becomes

$$H(\Omega)=\frac{\sum_{k=0}^{m}b_k e^{-jk\Omega}}{1+\sum_{k=1}^{n}a_k e^{-jk\Omega}} \quad (2)$$

or,

$$H(\Omega)=\frac{Y(\Omega)}{X(\Omega)}=\frac{b_0+b_1e^{-j\Omega}+b_2e^{-j2\Omega}+...+b_me^{-jm\Omega}}{1+a_1e^{-j\Omega}+a_2e^{-j2\Omega}+...+b_ne^{-jn\Omega}} \quad (3)$$

where $\Omega=2\pi\left(\frac{f}{f_s}\right)$ in [0, π] is the digital frequency; f is the analog frequency and f_s is the sampling frequency. Different fitness functions are used for IIR filter optimization problems [26-28]. The commonly used approach to IIR filter design is to represent the problem as an optimization problem with the mean square error (MSE) as the error fitness function [28] expressed in (4).

$$J(\omega)=\frac{1}{N_s}[(d(p)-y(p))^2] \quad (4)$$

where N_s is the number of samples used for the computation of the error fitness function; $d(p)$ and $y(p)$ are the filter's desired and actual responses. The difference $e(p)=d(p)-y(p)$ is the error between the desired and the actual filter response. The design goal is to minimize the MSE $J(\omega)$ with proper adjustment of coefficient vector ω represented as:

$$\omega=[a_0a_1...a_nb_0b_1...b_m]^T \quad (5)$$

In this paper, instead of (4), a novel error fitness function

given in (6) is adopted in order to achieve higher stop band attenuation and to have more control on the transition width. Using (6), it is found that the proposed filter design approach results in considerable improvement in stop band attenuation over other optimization techniques.

$$J_1(\omega) = \sum_{\omega} abs\left[abs\left(\left|H_d(\omega)\right| - 1\right) - \delta_p\right] + \sum_{\omega}\left[abs\left(\left|H_d(w)\right| - \delta_s\right)\right] \quad (6)$$

For the first term of (6), $\omega \in$ pass band including a portion of the transition band and for the second term of (6), $\omega \in$ stop band including the rest portion of the transition band. The portions of the transition band chosen depend on pass band edge and stop band edge frequencies.

The error fitness function given in (6) represents the generalized fitness function to be minimized using the evolutionary algorithms RGA, conventional PSO, and the proposed NPSO individually. Each algorithm tries to minimize this error fitness J_1 and thus optimizes the filter performance. Unlike other error fitness functions as given in [26-28] which consider only the maximum errors, J_1 involves summation of all absolute errors for the whole frequency band, and hence, minimization of J_1 yields much higher stop band attenuation and lesser pass band and stop band ripples.

III. Evolutionary Techniques Employed

Evolutionary algorithms stand upon the platform of heuristic optimization methods, which are characterized as stochastic, adaptive and learning in order to produce intelligent optimization schemes. Such schemes have the potential to adapt to their ever changing dynamic environment through the previously acquired knowledge. Few such efficient algorithms have been discussed for the purpose of designing as well as comparison of performances for handling the optimization problems of 6th and 8th order IIR LP and BP filters.

A. Real Coded Genetic Algorithm (RGA)

Standard Genetic Algorithm (also known as real coded GA) is mainly a probabilistic search technique, based on the principles of natural selection and evolution built upon the Darwin's "Survival of the Fittest" strategy [29]. Each encoded chromosome that constitutes the population is a solution to the filter designing optimization problem. These solutions may be good or bad, but are tested rigorously through the genetic operations such as crossover and mutation to evolve a global optimal or near global optimal solution to the problem at hand. Chromosomes are constructed over some particular alphabet {0, 1}, so that chromosomes' values are uniquely mapped onto the real decision variable domain. Each chromosome is evaluated by a function known as fitness function, which is usually the fitness function or objective function of the corresponding optimization problem. Each chromosome has a probability of selection and has to take part in the genetic operation based upon the Roulette's wheel strategy. In the genetic operations, crossover and mutation brings the variation in alleles of gene in the chromosome population along with the alleviation of trapping to local optimal solution.

Steps of RGA as implemented for the optimization of coefficient vector ω are as follows [30-33]:

Step 1: Initialize the real coded chromosome strings (ω) of n_p population, each consisting of equal number of numerator and denominator filter coefficients b_k and a_k, respectively; total coefficients = (n+1)*2 for nth order filter to be designed.

Step 2: Decoding the strings and evaluation of error fitness $J_1(\omega)$ according to (6).

Step 3: Selection of elite strings in order of increasing error fitness values from the minimum value.

Step 4: Copying the elite strings over the non selected strings.

Step 5: Crossover and mutation generate offsprings.

Step 6: Genetic cycle updating.

Step 7: The iteration stops when maximum number of cycles is reached. The grand minimum error fitness and its corresponding chromosome string or the desired optimal solution having (n+1)*2 number of coefficients are finally obtained.

B. Particle Swarm Optimization (PSO)

PSO is flexible, robust, population based stochastic search algorithm with attractive features of simplicity in implementation and ability to quickly converge to a reasonably good solution. Additionally, it has the capability to handle larger search space and non-differential objective function, unlike traditional optimization methods. Eberhart *et al.* [20-21] developed PSO algorithm to simulate random movements of bird flocking or fish schooling.

The algorithm starts with the random initialization of a swarm of individuals, which are known as particles within the multidimensional problem search space, in which each particle tries to move toward the optimum solution, where next movement is influenced by the previously acquired knowledge of particle best and global best positions once achieved by individual and the entire swarm, respectively. The features incorporated within this simulation are velocity matching of individuals with the nearest neighbour, elimination of ancillary variables and inclusion of multidimensional search and acceleration by distance. Instead of the presence of direct recombination operators, acceleration and position modification supplement the recombination process in PSO. Due to the aforementioned advantages and simplicity, PSO has been applied to different fields of practical optimization problems.

To some extent, IIR filter design with PSO is already reported in [15-18], [22-23]. A brief idea about the algorithm for a D-dimensional search space with n_p particles that constitute the flock is presented here. Each i^{th} particle is described by a position vector as: $S_i = (s_{i1}, s_{i2}, ..., s_{iD})^T$ and

a velocity vector as: $V_i = (v_{i1}, v_{i2}, ..., v_{iD})^T$.

The best position that the i^{th} particle has reached previously $pbest_i = (p_{i1}, p_{i2}, ..., p_{iD})^T$, and group best is expressed as $gbest = (p_{g1}, p_{g2}, ..., p_{gD})^T$.

The vectors of maximum and minimum velocities are $V_{\max}$, $V_{\min}$, respectively.

$V_{\max} = (v_{\max 1}, v_{\max 2}, ..., v_{\max D})^T$ and

$V_{\min} = (v_{\min 1}, v_{\min 2}, ..., v_{\min D})^T$.

The positive constants C_1, C_2 are related with accelerations and $rand_1, rand_2$ lie in the range [0, 1]. The inertia weight w is a constant chosen carefully to obtain fast convergence to optimum result. k denotes the iteration number.

The basic steps of the PSO algorithm are as follows [32]:

Step1: Initialize the real coded particles (ω) of n_p population, each consisting of equal number of numerator and denominator filter coefficients b_k and a_k, respectively; total coefficients D = (n+1)*2 for nth order filter to be designed.

Step 2: Compute the error fitness value for the current position S_i of each particle.

Step 3: Each particle can remember its best position $(pbest)$ which is known as cognitive information and that would be updated with each iteration.

Step 4: Each particle can also remember the best position the swarm has ever attained $(gbest)$ and is called social information and would be updated in each iteration.

Step 5: Velocity and position of each particle are modified according to (7) and (8), respectively [20].

$$V_i^{(k+1)} = w * V_i^{(k)} + C_1 * rand_1 * \{pbest_i^{(k)} - S_i^{(k)}\} + C_2 * rand_2 * \{gbest^{(k)} - S_i^{(k)}\} \quad (7)$$

where $V_i = V_{\max}$ for $V_i > V_{\max}$

$= V_{\min}$ for $V_i < V_{\min}$

$$S_i^{(k+1)} = S_i^{(k)} + V_i^{(k+1)} \quad (8)$$

Step 6: The iteration stops when maximum number of cycles is reached. The grand minimum error fitness and its corresponding particle or the desired solution having (n+1)*2 number of coefficients is finally obtained.

C. Novel Particle Swarm Optimization (NPSO)

The global search ability of conventional PSO is very much enhanced with the help of the following modifications. This modified PSO is termed as NPSO [34].

i) The two random parameters $rand_1$ and $rand_2$ of (7) are independent. If both are large, both the personal and social experiences are over used and the particle is driven too far away from the local optimum. If both are small, both the personal and social experiences are not used fully and the convergence speed of the technique is reduced. So, instead of taking independent $rand_1$ and $rand_2$, one single random number r_1 is chosen so that when r_1 is large, $(1-r_1)$ is small and vice versa. Moreover, to control the balance of global and local searches, another random parameter r_2 is introduced. For birds' flocking for food, there could be some rare cases that after the position of the particle is changed according to (7), a bird may not, due to inertia, fly toward a region at which it thinks is most promising for food. Instead, it may be leading toward a region which is in opposite direction of what it should fly in order to reach the expected promising regions. So, in the step that follows, the direction of the bird's velocity should be reversed in order for it to fly back into promising region. The term $sig\_m(r_3)$ is introduced for this purpose. Both cognitive and social parts are modified accordingly. Other medications are described below.

ii) A new variation in the velocity expression (7) is made by splitting the cognitive component (second part of (7)) into two different components. The first component can be called good experience component. That is, the particle has a memory about its previously visited best position. This component is exactly the same as the cognitive component of the basic PSO. The second component is given the name bad experience component. The bad experience component helps the particle to remember its previously visited worst position. The inclusion of the worst experience component in the behaviour of the particle gives additional exploration capacity to the swarm. By using the bad experience component, the bird (particle) can bypass its previous worst position and always try to occupy a better position.

Finally, with all modifications, the modified velocity of j^{th} component of i^{th} particle, replacing (7), is expressed as follows:

$$V_i^{(k+1)} = r_2 * sig\_m(r_3) * V_i^k + (1-r_2) * C_1 * r_1 * \{pbest_i^k - X_i^k\} + (1-r_2) * C_2 * (1-r_1) * \{gbest^k - X_i^k\} + (1-r_2) * C_1 * r_1 (X_i^k - pworst_i^k) \quad (9)$$

where $sig\_m(r_3)$ is a function defined as:

$$sig\_m(r_3) = -1 \quad when \quad r_3 \le 0.05$$
$$= +1 \quad when \quad r_3 > 0.05 \quad (10)$$

V_i^k is the velocity of i^{th} particle at k^{th} iteration; r_1, r_2 and r_3 are the random numbers between 0 and 1; X_i^k is the current position of i^{th} particle at k^{th} iteration; $pbest_i^k$ and $pworst_i^k$ are the personal best and the personal worst of i^{th} particle, respectively, at k^{th} iteration; $gbest^k$ is the group best among all $pbests$ for the group at k^{th} iteration. The

searching point in the solution space is as usual modified by the equation (8).

IV. Simulation Results and Discussions

Extensive MATLAB simulation study has been performed for performance comparison of three algorithms, RGA, PSO and NPSO for the 6th and 8th order IIR filter optimization problems. The design specifications followed for all algorithms are given in Table 1.

Table 1. Design Specifications of IIR LP and BP Filters

Type of Filter	Pass band ripple (δ_p)	Stop band ripple (δ_s)	Pass band normalized edge frequency (ω_p)	Stop band normalized edge frequency (ω_s)
LP	0.01	0.001	0.35	0.40
BP	0.01	0.001	0.35 and0.65	0.3 and 0.7

Table 2. Control parameters of RGA, PSO and NPSO

Parameters	RGA	PSO	NPSO
Population size	120	25	25
Iteration Cycle	100	100	100
Crossover rate	1	-	-
Crossover	Two Point Crossover	-	-
Mutation rate	0.01	-	-
Mutation	Gaussian Mutation	-	-
Selection Probability	1/3	-	-
C_1	-	2.05	2.05
C_2	-	2.05	2.05
v_i^{min}	-	0.01	0.01
v_i^{max}	-	1.0	1.0

The values of the control parameters of RGA, PSO and NPSO are given in Table 2. Each algorithm is run for 30 times to get the best solution of its own and all the best results are reported in this paper. All optimization programs were run in MATLAB 7.5 version on core (TM) 2 duo processor, 3.00 GHz with 2 GB RAM.

A. Analysis of Magnitude Response of IIR LP Filter

Three aspects of the algorithms are investigated in this work namely, their accuracy, speed of convergence and stability. Fig. 1 shows the comparative gain plots in dB for the designed 6th order IIR LP filter obtained for different algorithms. Fig. 2 represents the comparative normalized gain plots for 6th order IIR LP filter.

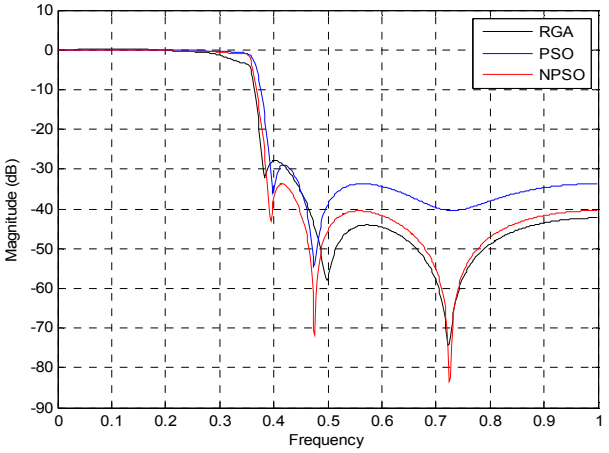

Fig. 1. Gain plots in dB for 6th order IIR LP filter using RGA, PSO and NPSO.

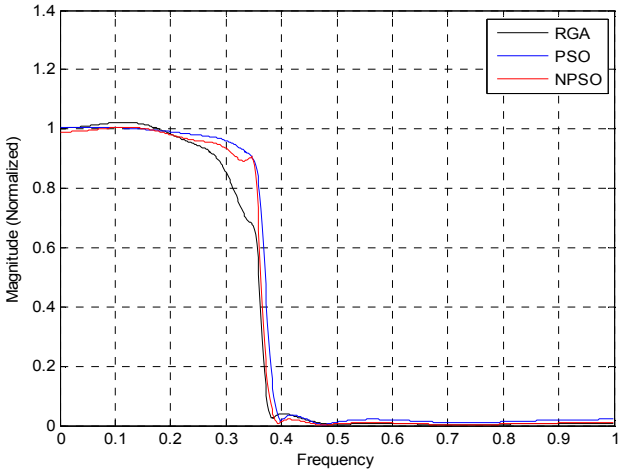

Fig. 2. Normalized gain plots for 6th order IIR LP filter using RGA, PSO and NPSO.

The best optimized numerator coefficients (b_k) and denominator coefficients (a_k) obtained after extensive simulation study are reported in Table 3. It is observed that maximum stop band attenuations 27.8345 dB, 28.94 dB and 33.7864 dB are obtained for RGA, PSO and NPSO algorithms, respectively. Gain plots and Tables IV and V also explore that the proposed 6th order IIR filter design approach using NPSO attains the highest stop band attenuation, the lowest stop band ripple with significantly small transition width and pass band ripple as compared to the results produced by RGA and PSO algorithms.

Figs. 3-5 show the pole-zero plots for 6th order IIR LP filter designed using RGA, PSO and NPSO, respectively. A system is called stable and minimum phase only when it's all poles and zeros, respectively, are within the unit circle of the z-plane. For designing the FIR filter, achieving these criteria is not a problem, but for IIR filters fulfilling these features simultaneously is really a challenging job. Fig. 3 shows the pole-zero plot of 6th order IIR LP filter designed with RGA.

In Fig. 4 pole-zero plot of 6th order IIR LP filter designed with PSO has been demonstrated. Fig. 5 shows the pole-zero plot of 6th order IIR LP filter designed with NPSO. In all these designs, stability is assured with the locations of all poles within the unit circle shown in Figs. 3-5.

Table 3. Optimized Coefficients and Performance Comparison of Different Algorithms for 6th order IIR LP Filter

Algorithms	Num. Coeff. (b_k)	Den. Coeff. (a_k)	Max. stop Band Attenuation (dB)
RGA	0.0334 0.0183 0.0691 0.0372 0.0675 0.0184 0.0330	1.0011 -2.7537 4.4663 -4.3975 -2.8654 -1.1215 0.2161	-27.8345
PSO	0.0729 0.0189 0.1405 0.0649 0.111 0.0388 0.0467	1.0007 -2.2202 3.3618 -2.9247 1.7854 -0.6235 0.1129	-28.94
NPSO	0.0379 0.0188 0.0772 0.0419 0.0766 0.0182 0.0372	1.0004 -2.6542 4.2439 -4.0895 2.6280 -1.0101 0.1925	-33.7864

Statistically and qualitatively analyzed data obtained from those graphs are presented in Tables 4-5, respectively. For IIR filter design, group delay is the function of normalized frequency due to which different frequency components undergo different amounts of phase shift. And the degree of severity increases as the distances of zeros are increased away from the unit circle. With this view point, Table 6 is prepared from Figs. 3-5 for the demonstration of closeness of crucial zeros to the perimeter of unit circle. It is to be noted that poles and zeros are situated symmetrically about the real part of z-plane so the radii of zeros and poles at the upper half are equal to those of the lower half.

It is observed from Table 6 that the zero Z_2 is just outside the unit circle along with two zeros Z_1 and Z_3 just inside the unit circle for RGA based design approach. For the PSO based design, it is noticed that the zero Z_1 stays outside the unit circle while the rest zeros are within the unit circle. But in the case of NPSO approach, a distinct point is explored about the position of zero Z_2 which is the closest to the boundary but just outside the circle along with rest of the zeros and poles which are clearly situated within the unit circle.

It can be concluded that positions of two zeros out of six are almost on the unit circle of z-plane for NPSO based design which gives the best group delay response among the others. In this paper the filter design is not limited to 6th order IIR filter but extended to 8th order filter also to verify the degree of superiority of higher order filter compared to its lower order version and to show the consistency in the superiority of the proposed NPSO. Fig. 6 shows the comparative gain plots in dB for the designed 8th order IIR LP filter obtained for different algorithms. Fig. 7 represents the comparative normalized gain plots for 8th order IIR LP filter. Statistically and qualitatively analyzed data obtained from those graphs are presented in Tables 7 and 8, respectively. Figs. 8-10 show the pole-zero plots for 8th order IIR LP filter designed using RGA, PSO and NPSO, respectively. Fig. 8 shows the pole-zero plot of 8th order IIR LP filter designed with RGA. In Fig. 9 pole-zero plot of 8th order IIR LP filter designed with PSO has been demonstrated. Fig. 10 shows the pole-zero plot of 8th order IIR LP filter designed with NPSO. In these designs also, stability is assured with the location of poles within the unit circle shown in Figs. 8-10. It has already been pointed out that the positions of zeros out side the unit circle affect the group delay criteria. From this view point Table 9 is prepared to demonstrate the radii of crucial zeros located close to unit circle. Conclusion can be made from the data represented in Table 9 that all the algorithms are capable enough to produce fair group delay responses due to the degree of closeness of zeros to the unit circle.

Gain plots as shown in Figs. 6-7 and Tables 7-8 reveal that for designing 8th order IIR LP filter the proposed algorithm NPSO outperforms the other optimization algorithms in terms of attaining the highest stop band attenuation, the lowest pass band and stop band ripple along with small transition width. Tables 4 and 7 also explore that the NPSO yields the highest value of mean attenuation, the least variance and the least standard deviation. The best optimized numerator coefficients (b_k) and denominator coefficients (a_k) obtained after extensive simulation study are reported in Table 10. It is observed that maximum stop band attenuations of 29.3896 dB, 30.5904 dB and 36.9916 dB are obtained for RGA, PSO and NPSO algorithms, respectively. Luitel *et al.* in [26] reported for 9th order IIR filter using PSO and DEPSO in which maximum attenuations of approximately 22dB and 25dB, respectively, have been reported. Luitel *et al.* reported the design of 9th order IIR filter using PSO and PSO-QI in [27] and approximate attenuations of 22dB and 27dB, respectively, have been reported. In this paper, maximum attenuation obtained for PSO is higher even though it is designed with lower order. In [28] Karaboga *et al.* has reported the design of 10th order minimum phase IIR filter using GA and the maximum attenuation of 14 dB (approx.) has been achieved.

Table 4.Statistical Data for Stop Band Attenuation (dB) for 6th order IIR LP Filter

Algorithm	Maximum	Mean	Variance	Standard Deviation
RGA	-27.8345	-38.0612	52.8107	7.2671

PSO	-28.9400	-32.1180	9.9952	3.1615
NPSO	-33.7864	-38.2573	5.0498	2.2472

Table 5. Qualitatively Analyzed Data for 6th order IIR LP Filter

Algorithm	Maximum Pass band Ripple (normalized)	Stop band ripple (normalized)			Transition Width (normalized)
		Maximum	Minimum	Average	
RGA	0.023	4.07×10^{-2}	1.94×10^{-4}	2.0432×10^{-2}	0.0493
PSO	0.004	3.59×10^{-2}	19.2×10^{-4}	1.8926×10^{-2}	0.0344
NPSO	0.005	2.06×10^{-2}	0.67×10^{-4}	1.0348×10^{-2}	0.0364

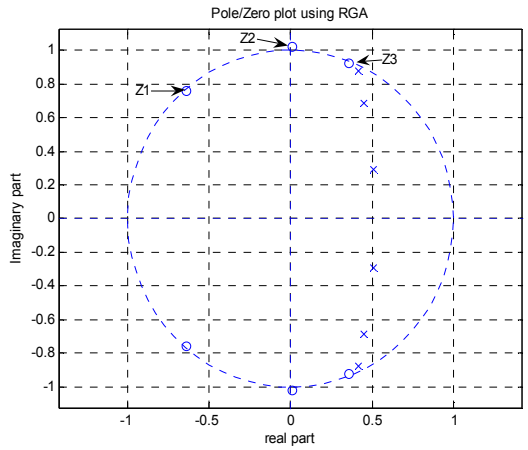

Fig. 3. Pole-Zero plot of 6th order IIR LP filter using RGA.

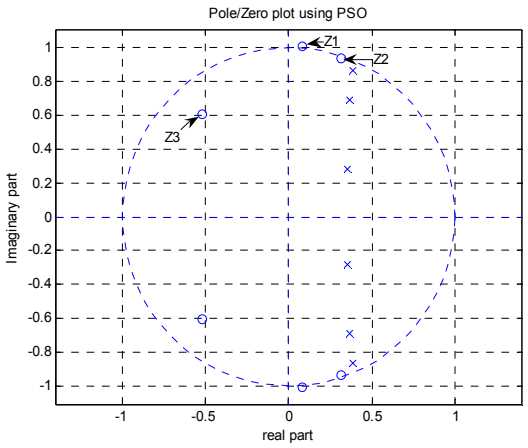

Fig. 4. Pole-Zero plot of 6th order IIR LP filter using PSO.

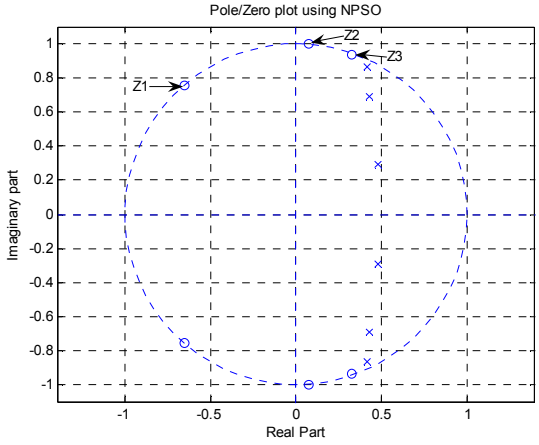

Fig. 5. Pole-Zero plot of 6th order IIR LP filter using NPSO.

Table 6. Radii of Zeros for 6th order IIR LP Filter

Algorithm	Zeros		
	Z1	Z2	Z3
RGA	0.98863	1.01963	0.98596
PSO	1.01035	0.98938	0.80075
NPSO	0.99856	1.00013	0.99202

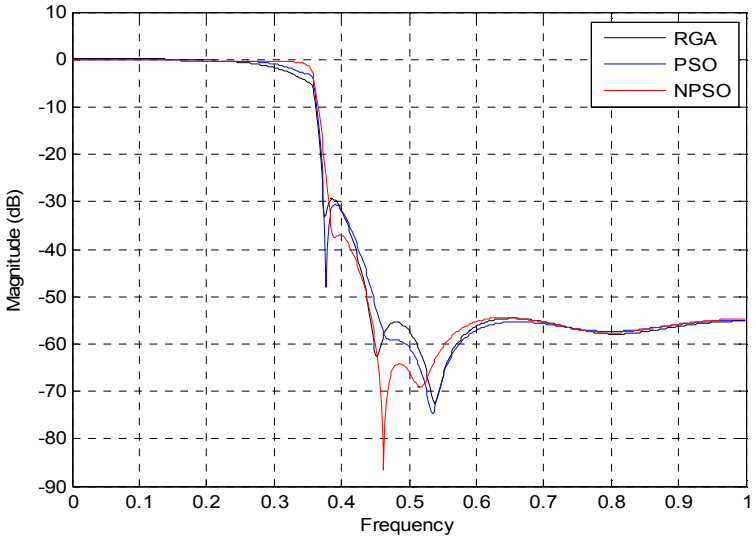

Fig. 6. Gain plots in dB for 8th order IIR LP filter using RGA, PSO and NPSO.

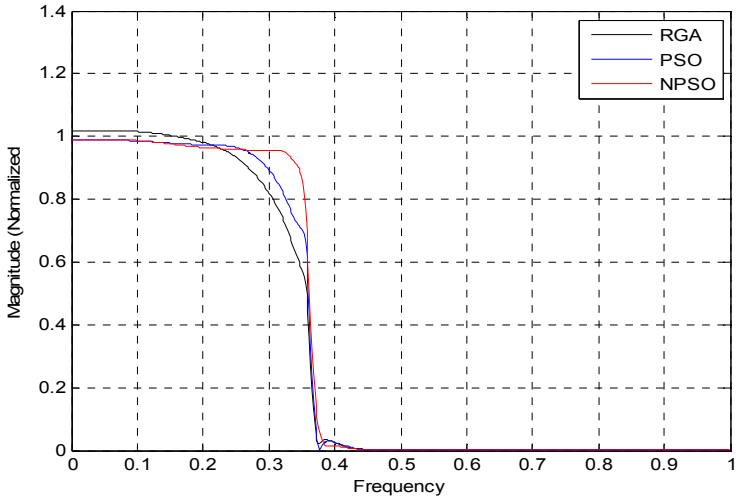

Fig. 7. Normalized gain plots for 8th order IIR LP filter using RGA, PSO and NPSO.

Table 7. Statistical Data for Stop Band Attenuation (dB) for 8th order IIR LP Filter

Algorithm	Maximum	Mean	Variance	Standard Deviation
RGA	-29.3896	-48.6365	123.5632	11.1159
PSO	-30.5904	-50.0187	128.6359	11.3418
NPSO	-36.9916	-52.5802	96.2146	9.8090

Table 8. Qualitatively Analyzed Data for 8th order IIR LP Filter

Algorithm	Maximum Pass band ripple (normalized)	Stop band ripple (normalized)			Transition Width (normalized)
		Maximum	Minimum	Average	
RGA	0.0182	3.39×10^{-2}	2.8235×10^{-4}	1.7091×10^{-2}	0.0481
PSO	0.0118	2.95×10^{-2}	1.8307×10^{-4}	1.4842×10^{-2}	0.0290
NPSO	0.0107	1.41×10^{-2}	0.4587×10^{-4}	0.7073×10^{-2}	0.0335

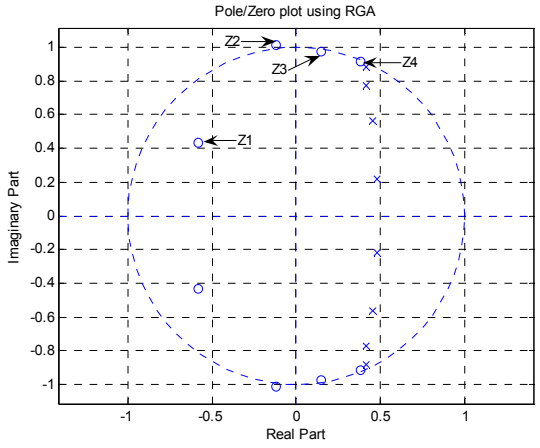

Fig. 8. Pole-zero plot of 8th order IIR LP filter using RGA.

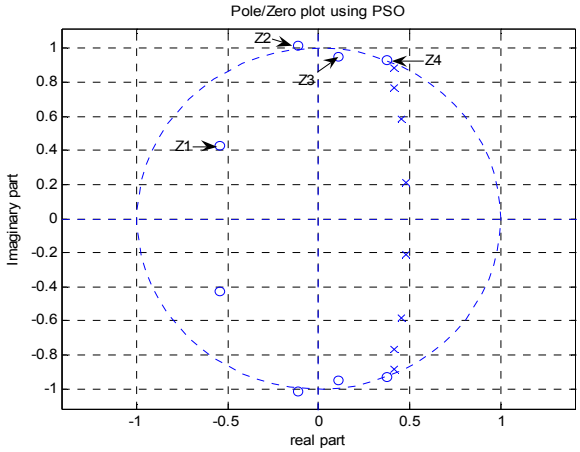

Fig. 9. Pole-zero plot of 8th order IIR LP filter using PSO.

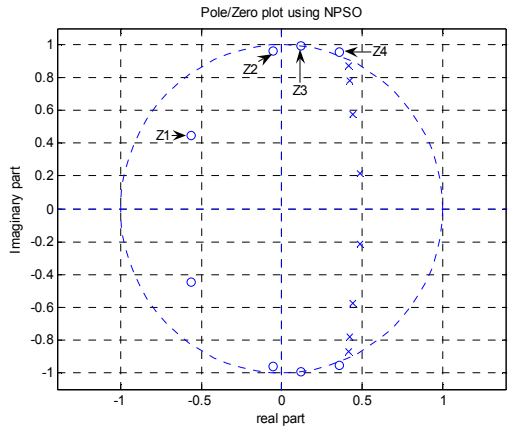

Fig. 10. Pole-zero plot of 8th order IIR LP filter using NPSO.

Table 9. Radii of Zeroes for 8th order IIR LP Filter

Algorithm	Zero			
	Z1	Z2	Z3	Z4
RGA	0.72524	1.02088	0.98347	0.99111
PSO	0.69360	1.02037	0.95481	1.00188
NPSO	0.72072	0.95981	1.00047	1.02191

Table 10. Optimized Coefficients and Performance Comparison of Different Algorithms for 8th order IIR LP filter

Algorithms	Num. Coeff. (b_k)	Den. Coeff. (a_k)	Max. stop Band Attenuation (dB)
RGA	0.0169 0.0059 0.0429 0.0239 0.0450 0.0299 0.0266 0.0120 0.0088	1.0004 -3.5211 7.1618 -9.4237 8.7904 -5.7900 2.6419 -0.7579 0.1064	-29.3896
PSO	0.0168 0.0058 0.0432 0.0228 0.0453 0.0286 0.0258 0.0115 0.0077	1.0001 -3.5200 7.1620 -9.4224 8.7896 -5.7890 2.6419 -0.7583 0.1061	-30.5904
NPSO	0.0165 0.0047 0.0428 0.0228 0.0451 0.0289 0.0268 0.0112 0.0082	1.0002 -3.5209 7.1635 -9.4234 8.7895 -5.7897 2.6427 -0.7595 0.1069	-36.9916

Table 19. Convergence Profile Data for RGA, PSO and NPSO for 8th order Low Pass IIR Filter

Algorithms	Minimum Error Value	Iteration Cycles	Convergence Speed (per cycle)	Execution time for 100 cycles (s)
RGA	3.988	100	2.903×10^{-2}	5.801761
PSO	3.019	100	4.135×10^{-2}	2.391630
NPSO	2.400	100	5.067×10^{-2}	3.969984

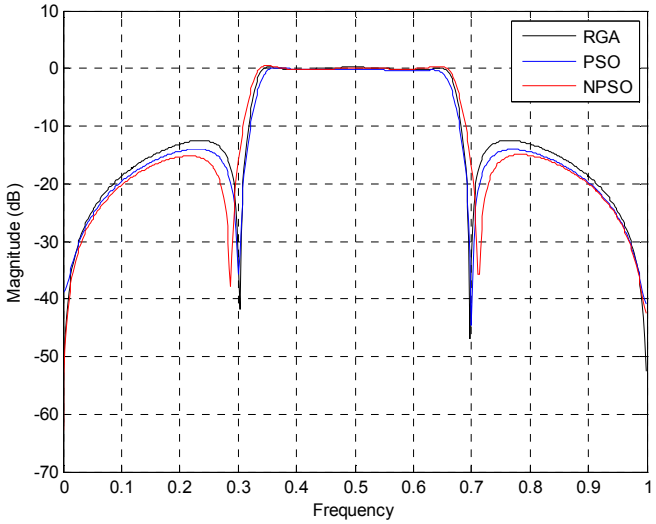

Fig. 11. Gain plots in dB for 6th order IIR BP filter using RGA, PSO and NPSO.

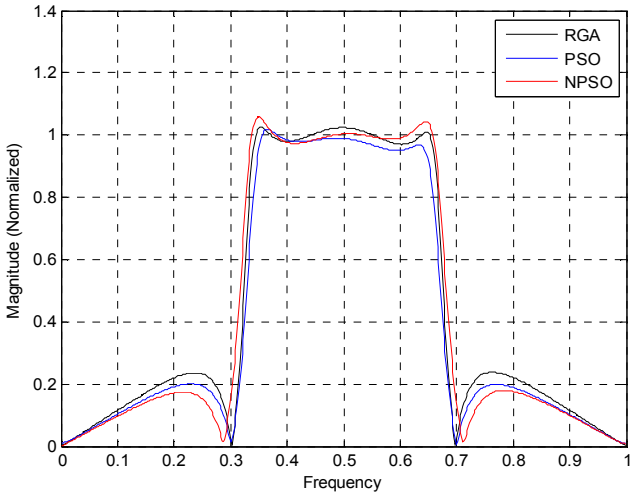

Fig. 12. Normalized gain plots for 6th order IIR BP filter using RGA, PSO and NPSO.

B. Analysis of Magnitude Responses of IIR Band Pass (BP) Filters

IIR BP filters of 6th and 8th orders are also designed with NPSO technique and results are compared with those of RGA and PSO for measuring the effectiveness of the proposed algorithm. Fig.11 shows the gain plots in dB for 6th order IIR BP filter using RGA, PSO and NPSO techniques. Normalized gain plots for 6th order IIR BP filter using RGA, PSO and NPSO techniques are shown in Fig. 12.

From these plots it can be perceived that the proposed NPSO algorithm obtains the highest stop band attenuation compared to the other mentioned optimization algorithms. The optimal filter coefficients are obtained by RGA, PSO and NPSO and are shown in Table 11. Table 12 shows the statistical performance of stop band attenuation obtained for 6^{th} order IIR BP filter. Table 12 depicts that the maximum attenuation of 14.9360 dB is attained for NPSO based IIR design with the highest mean attenuation and appreciably good consistence in results for variance and standard deviation. In Table 13, it is shown that the lowest stop band ripple is achieved for NPSO based design with small pass band ripple and transition width.

Pole-zero plots for the designed 6th order IIR BP filter are shown in Figs. 13-15 when RGA, PSO and NPSO are employed, respectively. From these plots it is evident that the designed 6th order BP filters are stable as the poles are located within the unit circle. Table 14 shows the radii of zeros which are calculated from Figs. 13-15.

In this section, optimal design of 8th order IIR BP filter is discussed. Fig. 16 shows the comparative gain plots in dB for the designed 8th order IIR BP filter obtained for different algorithms. Fig. 17 represents the comparative normalized gain plots for 8th order IIR BP filter. The best optimized numerator coefficients (b_k) and denominator coefficients (a_k) obtained

are reported in Table 15.

From Table 15 it is observed that maximum stop band attenuations of 18.2445 dB, 20.1389 dB and 21.7813 dB are obtained for RGA, PSO and NPSO algorithms, respectively. The gain plots as shown in Figs. 16-17 and Tables 16-17 explore that the proposed 8th order IIR filter design approach using NPSO results in the highest stop band attenuation, the lowest pass band and stop band ripples with significantly small transition width as compared to the results obtained when RGA and PSO algorithms are employed. Pole-zero plots obtained for the 8th order IIR filter designed using RGA, PSO and NPSO are shown in Figs. 18-20, respectively. From these plots it is evident that the designed 8th order BP filters are all stable due to the existence of poles within the unit circle. Table 18 shows the radii of zeros calculated from Figs. 18-20 for RGA, PSO and NPSO, respectively.

C. Comparative effectiveness and convergence profiles of RGA, PSO and NPSO

In order to compare the algorithms in terms of the error fitness values, Fig. 21 shows the convergences of error fitness values obtained by the algorithms. The convergence profiles are shown for the 8th order LP filter. Similar plots are also obtained for 6th order LP filter and both 6th and 8th order BP filters, which are not shown here.

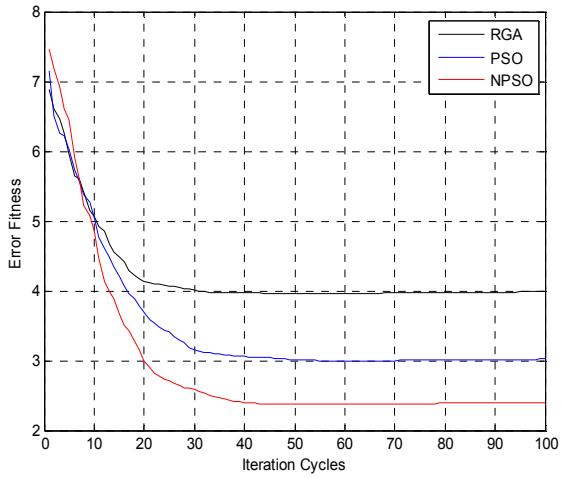

Fig. 21. Convergence profiles for RGA, PSO and NPSO for 8th order IIR LP filter.

As shown in Fig. 21, in case of 8th order LP filter, RGA converges to the minimum error fitness value of 3.988 in 5.801761 s; PSO converges to the minimum error fitness value of 3.019 in 2.391630 s; whereas, NPSO converges to the grand minimum error fitness value of 2.400 in 3.969984 s. The above-mentioned execution times may be verified from Table 19. Similar observations are made for 6th order LP filter also, which are not shown here. Table 19 summarizes the convergence profile data for the algorithms applied for the design of 8th order LP filter.

From Fig. 21 it can be concluded that the proposed algorithm NPSO obtains the minimum error fitness value as compared to PSO and RGA. It is also noticed that the proposed algorithm, NPSO has the faster rate of convergence in terms of sharp reduction in error fitness value shown in Fig. 21, compared to the rest error fitness function curves obtained by RGA and PSO algorithms for obtaining the optimum results. With a view to the above fact, it may finally be inferred that the performance of the NPSO is the best among all the mentioned algorithms.

V. Conclusions

In this paper, three different evolutionary optimization algorithms have been applied to the problems of designing 6th and 8th order low pass and band pass IIR digital filters. The filters thus obtained meet the stability criterion and show the best attenuation characteristics with reasonably good transition widths. Among the algorithms, the proposed NPSO yields the best attenuation characteristics and the best stop band ripples; converges very fast to the best quality optimal solution and reaches the lowest minimum error fitness value in moderately low execution time. Statistical results obtained for the NPSO also justify the potential of the proposed algorithm for the realization of IIR filters.

References

[1] A. V. Oppenheim and R. W. Buck, *Discrete-Time Signal Processing*, Prentice-Hall, NJ, 1999.

[2] J. G. Proakis and D. G. Manolakis, *Digital Signal Processing*, Prentice-Hall, NJ, 1996.

[3] M. C. Lang, "Least-squares design of IIR filters with prescribed magnitude and phase responses and pole radius constraint," *IEEE Trans. on Signal processing*, vol. 48, issue 11, pp. 3109-3121, Nov. 2000.

[4] L.B. Jackson and G. J. Lemay, "A simple Remez exchange algorithm to design IIR filters with zeros on the unit circle," *IEEE International Conference on Acoustics, Speech, and Signal Processing*, USA, vol. 3, pp. 1333-1336, 1990.

[5] Z. M. Hussain, A. Z. Sadik and P. O'Shea, "*Digital Signal Processing-An Introduction with MATLAB Applications*," Springer-Verlag, 2011.

[6] A. Antoniou, "*Digital Signal Processing: Signals, Systems and Filters*," McGraw Hill, 2005.

[7] W. S. Lu and A. Antoniou, "Design of digital filters and filter banks by optimization: a state of the art review", in *Proc. European Signal Processing Conf*., vol. 1, pp. 351-354, Finland, Sep. 2000.

[8] J. T. Tsai, J. H. Chou and T. K. Liu, "Optimal design of digital IIR filters by using hybrid Taguchi genetic algorithm," *IEEE Trans. on Industrial Electronics*, vol. 53, no. 3, pp. 867-879, 2006.

[9] Y. Yu and Y. Xinjie, "Cooperative co-evolutionary genetic algorithm for digital IIR filter design," *IEEE Trans. on Industrial Electronics*, vol. 54, no. 3, pp. 1311-1318, 2007.

[10] S. Chen, R. Istepanian and B. L. Luk, "Digital IIR filter design using adaptive simulated annealing," *Digital Signal Processing*, vol. 11, no. 3, pp. 241-251, 2001.

[11] A. Kalinli and N. Karaboga, "Artificial immune algorithm for IIR filter design," *Engineering Applications of Artificial Intelligence*, vol. 18, no. 8, pp. 919-929, 2005.

[12] N. Karaboga, A. Kalinli and D. Karaboga, "Designing digital IIR filters using ant colony optimization algorithm," *Engineering Applications of Artificial Intelligence*, vol. 17, no. 3, pp. 301-309, 2004.

[13] N. Karaboga and M. H. Cetinkaya, "A novel and efficient algorithm for adaptive filtering: artificial bee colony algorithm," *Turk. J. Elec. Eng and Comp Sci*, 19, (1), pp. 175-190, 2011.

[14] G. Panda, P. M. Pradhan and B. Majhi, "IIR system identification using cat swarm optimization," *Expert Systems with Applications*, vol. 38, no. 10, pp. 12671-12683, 2011.

[15] S. T. Pan and C. Y. Chang, "Particle swarm optimization on D-stable IIR filter design," *IEEE World Congress on Intelligent Control Automation*, WCICA '11, Taipei, pp. 621-626, 2011.
[16] S. Das and A. Konar, "A swarm intelligence approach to the synthesis of two-dimensional IIR filters," *Engineering Applications of Artificial Intelligence*, vol. 20, no. 8, pp. 1086-1096, 2007.
[17] W. Fang, J. Sun and W. Xu, "A new mutated quantum-behaved particle swarm optimization for digital IIR filter design," *EURASIP Journal on Advances in Signal Processing*, pp. 1-7, 2009.
[18] Y. Gao, Y. Li and H. Qian, "The design of IIR digital filter based on chaos particle swarm optimization algorithm," *IEEE Int. Conf. on Genetic and Evolutionary Computing*, pp. 303-306.
[19] J. H. Holland, *"Adaptation in Natural and Artificial Systems,"* Ann Arbor, MI: Univ. Michigan Press. 1975.
[20] J. Kennedy and R. Eberhart, "Particle swarm optimization," in *Proc. IEEE Int. Conf. On Neural Network*, vol. 4, pp. 1942-1948, 1995.
[21] R. Eberhart and Y. Shi, "Comparison between genetic algorithm and particle swarm optimization," in *Evolutionary Programming VII*, pp. 611-616, Springer, 1998.
[22] J. Sun, W. Fang and W. Xu, "A quantum-behaved particle swarm optimization with diversity-guided mutation for the design of two-dimensional IIR digital filters," *IEEE Trans. on Circuits and Systems-II*, vol. 57, no. 2, pp. 141-145, Feb. 2010.
[23] S. Chen and B. L. Luk, "Digital IIR filter design using particle swarm optimization," *Int. J. Modelling, Identification and Control,* vol. 9, no. 4, pp. 327-335, 2010.
[24] S. H. Ling, H. H. C. Iu, F. H. F. Leung and K. Y. Chan, "Improved hybrid particle swarm optimized wavelet neural network for modelling the development of fluid dispensing for electronic packaging," *IEEE Trans. Ind. Electron*., vol. 55, no. 9, pp. 3447-3460, Sep. 2008.
[25] B. Biswal, P. K. Dash and B. K. Panigrahi, "Power quality disturbance classification using fuzzy c-means algorithm and adaptive particle swarm optimization," *IEEE Trans. Ind. Electron.*, vol. 56, no. 1, pp. 212-220, Jan. 2009.
[26] B. Luitel and G. K. Venayagamoorthy, "Differential evolution particle swarm optimization for digital filter design," *IEEE Congress on Evolutionary Computation*, pp. 3954-3961, 2008.
[27] B. Luitel and G. K. Venayagamoorthy, "Particle swarm optimization with quantum infusion for the design of digital filters," *IEEE Swarm Intelligence Symposium*, St. Louis, MO USA, pp. 1-8, Sept. 2008.
[28] N. Karaboga and B. Cetinkaya, "Design of minimum phase digital IIR filters by using genetic algorithm," in *Proc. IEEE 6th Nordic Signal Processing Symposium* 2004, Finland, pp. 29-32, June.
[29] J. H. Holland, *Adaptation in Natural and Artificial Systems*, Ann Arbor, MI: Univ. Michigan Press. 1975.
[30] D. Mondal, S. P. Ghosal and A. K. Bhattacharya, "Radiation pattern optimization for concentric circular antenna array with central element feeding using craziness based particle swarm optimization," *International Journal of RF and Microwave Computer-Aided Engineering*, 20(5): 577-586, Sept. 2010.
[31] D. Mondal, S. P. Ghosal and A. K. Bhattacharya, "Application of evolutionary optimization techniques for finding the optimal set of concentric circular antenna array," *Expert Systems with Applications*, 38, pp. 2942-2950, 2010.
[32] S. Mandal, S. P. Ghoshal, R. Kar, D. Mandal, "Optimal Linear Phase FIR Band Pass Filter Design using Craziness Based Particle Swarm Optimization Algorithm", *Journal of Shanghai Jiaotong University (Science)*, Springer, Vol. 16, No. 6, pp. 696-703, 2011.
[33] S. Mandal, S. P. Ghoshal, R. Kar, D. Mandal, "Design of Optimal Linear Phase FIR High Pass Filter using Craziness based Particle Swarm Optimization Technique" *Journal of King Saud University – Computer and Information Sciences*, Elsevier, vol. 24, pp. 83–92, 2012.
[34] D. Mandal, S. P. Ghoshal, and A. K. Bhattacharjee, "Wide Null Control of Symmetric Linear Antenna Array Using Novel Particle Swarm Optimization," *International Journal of RF and Microwave Computer-Aided Engineering*, vol. 21, no. 4, pp. 376-382, Apr. 2011.